

# TtOmp85, a $\beta$ -Barrel Assembly Protein, Functions by Barrel Augmentation

Luisa Estrada Mallarino,<sup>†</sup> Enguo Fan,<sup>‡</sup> Meike Odermatt,<sup>†</sup> Matthias Müller,<sup>‡</sup> MeiShan Lin,<sup>§</sup> Jie Liang,<sup>§</sup> Martin Heinzelmann,<sup>†</sup> Fenja Fritsche,<sup>†</sup> Hans-Jürgen Apell,<sup>†</sup> and Wolfram Welte<sup>\*,†</sup>

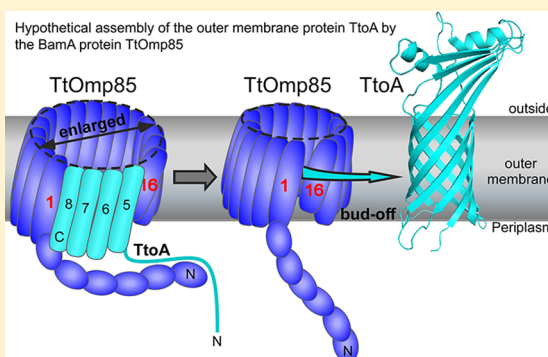
<sup>†</sup>Department of Biology, University of Konstanz, Universitätsstraße 10, 78457 Konstanz, Germany

<sup>‡</sup>Institute of Biochemistry and Molecular Biology, ZBMZ, University of Freiburg, Stefan-Meier-Straße 17, 79104 Freiburg im Breisgau, Germany

<sup>§</sup>Department of Bioengineering, MC 063, University of Illinois at Chicago, 851 South Morgan Street, Room 218, Chicago, Illinois 60607, United States

## S Supporting Information

**ABSTRACT:** Outer membrane proteins are vital for Gram-negative bacteria and organisms that inherited organelles from them. Proteins from the Omp85/BamA family conduct the insertion of membrane proteins into the outer membrane. We show that an eight-stranded outer membrane  $\beta$ -barrel protein, TtoA, is inserted and folded into liposomes by an Omp85 homologue. Furthermore, we recorded the channel conductance of this Omp85 protein in black lipid membranes, alone and in the presence of peptides comprising the sequence of the two N-terminal and the two C-terminal  $\beta$ -strands of TtoA. Only with the latter could a long-living compound channel that exhibits conductance levels higher than those of the Omp85 protein alone be observed. These data support a model in which unfolded outer membrane protein after docking with its C-terminus penetrates into the transmembrane  $\beta$ -barrel of the Omp85 protein and augments its  $\beta$ -sheet at the first strand. Augmentation with successive  $\beta$ -strands leads to a compound, dilated barrel of both proteins.



The correct and controlled assembly of membrane proteins is a prerequisite for cell viability. Outer membrane proteins (OMPs) have to be assembled without free energy sources and are predominantly up and down  $\beta$ -barrel proteins.<sup>1</sup> Unassisted insertion of barrel proteins into membranes *in vitro* has been observed,<sup>2</sup> but the low efficiency points to the need of reducing the energetic barrier of translocation of the polar extracellular OMP loops, doubtlessly one of the basic functions of the OMP insertases of the Omp85 family identified in the Tommassen group.<sup>3</sup> In both prokaryotes and eukaryotes, members of the Omp85 family were found to be essential for cell viability.<sup>4</sup> The absence of Omp85 leads to the accumulation of OMPs in the periplasm, suggesting that the cell is unable to assemble them in functional form in the outer membrane.<sup>3</sup>

Struyvé et al.<sup>5</sup> proposed that the C-terminal hydrophobic residues, particularly the conserved C-terminal phenylalanine, play a role in the assembly of OMPs. This C-terminal recognition sequence was found to be critical for the recognition of unfolded OMPs by Omp85 proteins.<sup>6,7</sup>

Omp85 proteins possess a C-terminal membrane-inserted  $\beta$ -barrel domain consisting of 16 antiparallel  $\beta$ -strands. N-Terminally, they possess between one and six POTRA (polypeptide transport-associated) domains, each with 75 residues on average, which contribute to the insertase activity.<sup>8,9</sup> In *Escherichia coli*, five POTRA domains form the N-terminus of the Omp85

ortholog BamA (Bam stands for  $\beta$ -barrel assembly machine), formerly designated YaeT. The observation that the POTRA domain preceding the barrel domain is essential for the insertase function of Omp85<sup>10</sup> suggested that the unfolded substrate OM protein first docks to a POTRA domain rather than binding directly to the barrel domain. Recently, three structures of Omp85 insertases have been reported.<sup>11,12</sup>

Sequence homology and physicochemical properties suggested to us<sup>13</sup> the existence of an Omp85 ortholog in *Thermus thermophilus* that we call TtOmp85 in this study. This protein has been overexpressed, isolated, and biochemically characterized. Reconstituted in black lipid membranes, it forms ion channels with single-channel conductances of  $\sim 0.4$  and  $\sim 0.65$  nS.<sup>13</sup> The assembly of OMPs in this ancestral thermophilic eubacterium<sup>14</sup> attracted our interest because we expected to encounter a rudimentary system, less sophisticated and more thermotolerant than those in the phylogenetically younger mesophilic Gram-negative bacteria. In previous work, we showed that unfolded TtoA, a major outer membrane protein of *T. thermophilus*, acts as bait for TtOmp85.<sup>6</sup> When a TtoA fragment lacking the nine

Received: September 8, 2014

Revised: November 20, 2014

Published: December 22, 2014

C-terminal residues that are known to act as the recognition sequence for insertases of the Omp85 family was used,<sup>7</sup> the interaction with TtOmp85 was absent.

The data that we present here show that TtOmp85 shares a weak energy of barrel closure with other BamA proteins that, however, is not found in other outer membrane proteins. Moreover, we directly show TtOmp85-assisted insertion and folding of TtoA into liposomes. Finally, we present conductance data of TtOmp85 in black lipid membranes showing channel alterations in the presence of TtoA-derived peptides consistent with formation of a compound  $\beta$ -barrel protein by  $\beta$ -augmentation of the opened TtOmp85 barrel by these peptides.

## ■ EXPERIMENTAL PROCEDURES

**Topology Prediction of the TtOmp85 Barrel Domain and Its Interstrand Energies.** Transmembrane  $\beta$ -strands of TtOmp85 were predicted from sequence using three servers, Pred-TMBB,<sup>15</sup> TMBETAPRED,<sup>16</sup> and Psi\_Pred.<sup>17</sup> Further adjustment of TM strand assignments was based on the comparison with TM strands of three Omp85 family proteins with known three-dimensional (3D) structures.<sup>11,12</sup>

The hydrogen bonding pattern between the  $\beta$ -strands of the TtOmp85 barrel was predicted using an empirical energy function.<sup>18,19</sup>

The interaction energy between the first and 16th strands of TtOmp85 was calculated according to the simplified strand-strand interaction model<sup>18</sup> using the predicted TM region topology. The calculation of the interaction energy value (in kT units) was performed as described using an empirical potential function TMSIP derived from a set of  $\beta$ -barrel membrane proteins.<sup>18</sup> In our model, each residue interacts with two residues in the neighboring strand through strong H-bond interactions, side-chain interactions, or weak H-bond interactions.<sup>20</sup> The interaction energy between two strands is the summation of the residue-residue interaction energy over all residues in these strands. All possible configurations of two neighboring strands were enumerated using a model of reduced discrete state space.<sup>19</sup> The standard error of strand interaction energy was calculated from the population variance of values of interaction energy of these enumerated configurations. For the three Omp85 family proteins and five porins with known 3D structures,<sup>11,12</sup> the interaction energy of the first and 16th strands was calculated on the basis of their available structures.

**Bacterial Strains and Growth Conditions.** TtOmp85 with an N-terminal Strep tag and TtoA with an N-terminal His tag were expressed in *T. thermophilus* HB27 cells transformed with derivatives of plasmid pMK18 as described previously.<sup>13,21</sup> Growth of transformed bacteria was performed according to the method described in ref 13. In brief, *T. thermophilus* was grown at 70 °C in autoclaved medium containing 8 g/L Trypticase, 4 g/L yeast extract, and 3 g/L NaCl dissolved in distilled water (pH 7.5) supplemented with 100  $\mu$ g/mL kanamycin. The protein was constitutively expressed.

**Purification of Strep-TtOmp85 and His-TtoA.** All percent concentrations are given as w/v herein. For TtOmp85, cell pellets of *T. thermophilus* were resuspended in buffer H [20 mM Tris, 1 mM EDTA, 100 mM NaCl, and 20% glycerol (pH 7.5)] mixed with DNase I and one protease inhibitor cocktail tablet (Roche) and disrupted by being passed three times through a French pressure cell (G. Heinemann, Schwäbisch Gmünd, Germany) at 16000 psi. Cell envelopes were obtained by centrifugation of the suspension at 100000g and 4 °C for 1 h. The crude membrane pellet resuspended in buffer H was shock-frozen in

liquid nitrogen and stored at -80 °C or directly used for solubilization.

Membranes were solubilized in 1% Cymal-6 (Anatrace) for 1 h at 37 °C under mild agitation, followed by centrifugation at 36000g and incubation at 4 °C for 1 h. The supernatant was mixed with preequilibrated streptactin sepharose beads (GE Healthcare) at a ratio of 75  $\mu$ L of beads per milliliter of supernatant and incubated for at least 1 h at 37 °C under mild agitation to achieve binding of Strep-TtOmp85.

The samples were centrifuged at 4400g for 5 min. The supernatant was discarded, and the beads were washed twice with buffer A [20 mM Tris (pH 7.5), 1 mM EDTA, 100 mM NaCl, and 0.05% Cymal-6]. After addition of buffer B (buffer A with 2.5 mM desthiobiotin), the sample was incubated again under the same conditions as previously described. After another centrifugation at 4400g for 5 min, the supernatant containing the eluted Strep-TtOmp85 was concentrated with a 50 kDa Vivaspin concentrator, filtered through a 0.45  $\mu$ m centrifugal filter, and applied to a Superdex 200 HR 10/30 column equilibrated in buffer A. A solution of 0.1 mg/mL TtOmp85 in protein buffer [20 mM Tris, 100 mM NaCl, and 0.05% Cymal-6 (pH 8.5)] was used for reconstitution into liposomes and BLM assays.

The purified Strep-TtOmp85 was stored at 4 °C for a maximum of 3 weeks.

The protein purity was checked with sodium dodecyl sulfate-polyacrylamide gel electrophoresis (SDS-PAGE) analysis according to the method described in ref 22. The protein concentration was determined by the bicinchoninic acid (BCA) method.<sup>23</sup>

His-TtoA was purified as described in ref 21.

In the following, the proteins will be termed TtOmp85 and TtoA, respectively.

**In Vitro Integration of TtoA into TtOmp85 Proteoliposomes.** To synthesize TtoA as a radioactively labeled substrate for *in vitro* integration experiments, an S135-based cell-free protein synthesis system of *E. coli* was used. S135 is a cytosolic cell extract that was prepared from the *E. coli* Top10 strain (Invitrogen) according to the method described in ref 24. It allows the expression of proteins by coupled transcription/translation from plasmid-encoded genes. *In vitro* synthesis of a signal sequence-less version of TtoA from plasmid pET28-HisTtoA<sup>6</sup> was performed at 37 °C for 20 min as described previously.<sup>24</sup>

TtOmp85-containing proteoliposomes (100  $\mu$ L) were prepared from 1.5  $\mu$ g of purified TtOmp85 according to the method described in ref 25. An aliquot of 20  $\mu$ L of proteoliposomes was combined with 30  $\mu$ L of *in vitro* synthesized TtoA to perform *in vitro* integration at 37 or 70 °C for 15 min. The proteoliposomes were pelleted at 186000g<sub>max</sub> for 30 min at 4 °C in a Beckman TLA-55 rotor, and the pellet was resuspended in 48  $\mu$ L of INV buffer [50 mM triethanolamine acetate (pH 7.5), 250 mM sucrose, and 1 mM dithiothreitol] and supplemented with 12  $\mu$ L of 5 $\times$  SDS loading buffer.<sup>24</sup> One aliquot (30  $\mu$ L) was treated at 95 °C for 5 min while being shaken at 14000 rpm, whereas the other aliquot was directly loaded on a 15% SDS-polyacrylamide gel.

**Single-Channel Conductance across Black Lipid Membranes.** L-1,2-Diphytanoyl-3-phosphatidylcholine (PhPC) was obtained from Avanti Polar Lipids, Inc. (Alabaster, AL). All other reagents were of at least analytical grade.

Optically black lipid membranes (BLM) were formed from a solution of 10 mg/mL PhPC in *n*-decane.<sup>26</sup> The membrane cell was made of Teflon and enclosed in a thermostated metal block

( $T = 20 \pm 2$  °C). The septum between both compartments had a circular hole  $\sim 0.2$  mm in diameter. The solutions on both sides of the BLM were connected to the external measuring circuit via silver/silver chloride electrodes. The membrane voltage was 100 mV throughout. The single-channel conductance of TtOmp85 solubilized in Cymal-6 was determined in buffer containing 10 mM Tris, 5 mM CaCl<sub>2</sub>, 1 M KCl, and 0.05% Cymal-6 (pH 7.4). After a stable bilayer had been obtained, the solubilized protein was added to the rear compartment (volume of 2 mL). To obtain only a single active ion channel at the same time, a typical addition was 3  $\mu$ L of 0.1 mg/mL TtOmp85 in 20 mM Tris, 100 mM NaCl, and 0.05% Cymal-6 (pH 8.5). Single-channel events were detected after various periods of time. The lifetime of the BLM was >30 min. When the BLM broke, another bilayer was immediately formed in the same buffer.

Current measurements were performed in a Faraday cage using an operational amplifier with a feedback resistance,  $R_F$ , of  $10^{10}$   $\Omega$  and a time resolution of 1 ms. Traces with single-channel currents were recorded with an analog–digital converter (National Instruments, NI USB-6341), processed with LabVIEW, and stored in files with a sampling frequency of 1 kHz.

To analyze the single-channel events, histograms of conductance transitions were determined. The background current of pure BLM was  $\sim 2$ – $5$  pA with a current noise of  $\sim 5$  pA. Single-channel currents frequently showed rapid fluctuations below 1 nA in the millisecond time range. The software evaluated only current transitions of >1 nA as conductance transitions of the ion channels. These events were compiled in histograms of the channel conductance transitions. For this purpose, the respective current amplitudes were divided by the applied membrane potential of 100 mV.

**TtoA-Derived Peptides and Conductance Recordings of TtOmp85 in Black Lipid Membranes.** Using the coordinates of TtoA,<sup>6</sup> four synthetic peptides were designed: B1 comprising the 18 N-terminal residues (MAAKFSVEAGA-GFYGGFG) forming the first  $\beta$ -strand, B1-2 comprising the 32 N-terminal residues (MAAKFSVEAGAGFYGGFGQLAVVA-EDLAPGL) forming the first two  $\beta$ -strands, B7-8 comprising the 65 C-terminal residues 142–207 (NLSLVGDLGVDYFQAC-FTRVEEDDSGNKSQSSVCPGDSGYEDVNKFVTPQPEWV-LKRLGAAAYRF) forming the seventh and eighth  $\beta$ -strands, and B8 comprising the 17 C-terminal residues 190–207 (TQPEW-VLKLRLGAAAYRF) containing the residues forming the eighth  $\beta$ -strand of TtoA (see Figure 2 of the Supporting Information). The lyophilized peptides were supplied as trifluoroacetate salts by Peptide2.0 (Chantilly, VA). The purity was >96%, as confirmed by high-performance liquid chromatography.

BLM experiments were performed to measure and analyze the effect of the peptides on the single-channel properties of TtOmp85. The measurements were performed as described above. The only difference was that before the addition of the protein–peptide combinations the protein was mixed with a 5-fold excess of one of the peptides, B8, B7-8, B1, or B1-2. All peptides were dissolved at a concentration of 0.1 mg/mL in 20 mM Tris, 100 mM NaCl, and 0.05% Cymal-6 (pH 8.5). Control experiments were performed in the absence of TtOmp85 either with the detergent only (0.05% Cymal-6) or with 3  $\mu$ L of one of the peptide solutions.

## RESULTS

**TtOmp85 and Other Members of the Omp85 Family Have Low Barrel-Closure Energies.** The structures of BamA and TamA suggest that the barrel-closure energies, i.e., the

interaction between barrel  $\beta$ -strand 1 and  $\beta$ -strand 16, are particularly weak. To determine if this is a general property of Omp85 proteins that is not found in other 16-stranded transmembrane  $\beta$ -barrels, we calculated the barrel-closure energies on a relative scale of some representatives of Omp85 proteins and of general diffusion porins of known structure. To include TtOmp85, a topology model of Omp85 proteins was made (see Experimental Procedures) (see Figure 1 of the Supporting Information). The shear number of the predicted TtOmp85  $\beta$ -barrel topology was 20, which is in the same range as that of TamA<sup>12</sup> [Protein Data Bank (PDB) entry 4C00].

As shown in Figure 1 and Table 1 of the Supporting Information, the interaction energy of the first and 16th strands

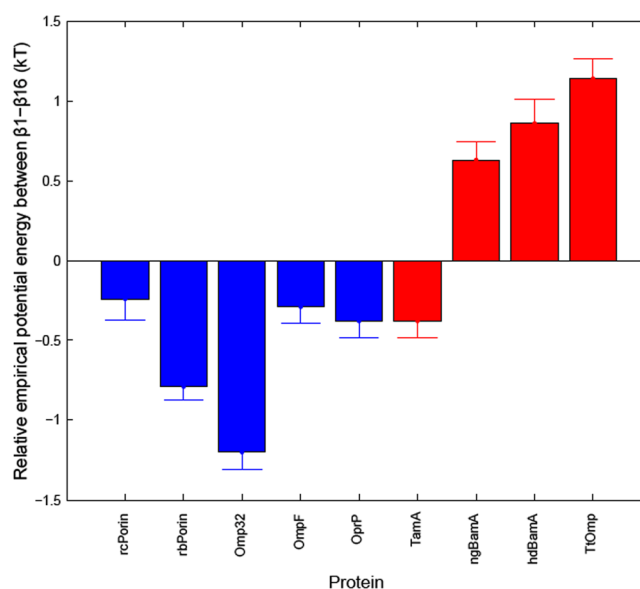


**Figure 1.** Barrel-closure energies. Interaction energies (in kT units) of the first and 16th strands are calculated using statistical potential energy scale TMSIP for five proteins from the porin family (blue) and four proteins from the Omp85 family (red). The PDB entries of the porins are 2POR (porin from *Rhodobacter capsulatus*), 1PRN (porin from *Rhodospseudomonas blastica*), 2OMF (OmpF from *E. coli*), 1E54 (Omp32 from *Comamonas acidophorans*), and 2O4V (OprP from *Pseudomonas aeruginosa*). The Omp85 family proteins are 4C00 (TamA from *E. coli*), 4K3B (BamA from *N. gonorrhoeae*), 4K3C (BamA from *H. ducreyi*), and TtOmp85 (no structure available; the calculation is based on the topology prediction of the transmembrane region given in Figure 1 of the Supporting Information).

in BamA from *Neisseria gonorrhoeae* and *Haemophilus ducreyi* and in TtOmp85 was significantly more positive than the corresponding energy in the porin family, indicating that the barrel-closure energy in the Omp85 family is relatively weak and less costly to disrupt than in porins.

**TtOmp85 Expression in *T. thermophilus*.** TtOmp85 harboring an N-terminal Strep tag was expressed in *T. thermophilus* HB27 using the vector pMK18 (see Experimental Procedures) and purified from a Cymal-6-solubilized membrane fraction using streptactin sepharose. The eluate shows a single band at an apparent molecular mass of 80 kDa corresponding to Strep-TtOmp85 (Figure 2A). Size-exclusion chromatography was performed as a final purification step.

The identity of the purified protein was confirmed as TtOmp85 via peptide fragment mass spectrometry (PF-MS).

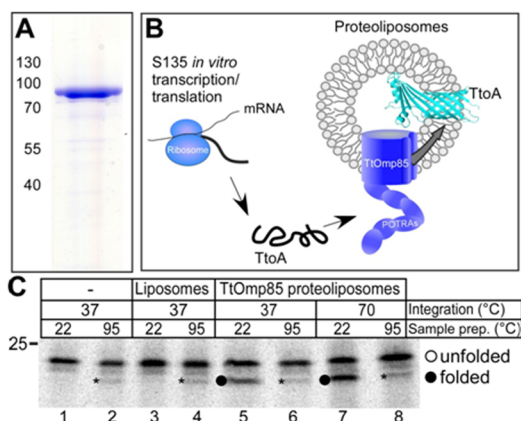


**Figure 2.** TtOmp85 purified from *T. thermophilus* and reconstituted into proteoliposomes is functionally active. (A) The purified protein migrates as a single band at an apparent molecular mass of 80 kDa. (B) Scheme of the experimental setup to show TtOmp85-assisted insertion and folding of *in vitro*-synthesized TtoA into proteoliposomes. (C) <sup>35</sup>S-labeled TtoA synthesized *in vitro* and incubated at 37 or 70 °C with the indicated vesicles is displayed by SDS–PAGE and visualized by phosphoimaging. Treatment with SDS sample buffer was performed at 22 or 95 °C. At the lower temperature, the structure of correctly folded TtoA is preserved (black dot). The origin of the band labeled with an asterisk is not known.

**Purified TtOmp85 Reconstituted into Proteoliposomes Promotes Insertion and Compact Folding of TtoA in the Membrane.**

The gene encoding the *T. thermophilus*  $\beta$ -barrel outer membrane protein TtoA was expressed *in vitro* from plasmid pET28-HisTtoA using an *E. coli* S135 cell extract as the transcription/translation system as outlined in Figure 2B. TtOmp85 purified as described above was reconstituted with *E. coli* phospholipids into proteoliposomes following a previously published protocol.<sup>25</sup> The TtOmp85-containing proteoliposomes were then incubated with *in vitro*-synthesized TtoA at 37 or 70 °C for 15 min (Figure 2B) and thereafter collected by high-speed centrifugation. The pellet was resuspended in INV buffer and supplemented with SDS–PAGE loading buffer. Samples were split in half, and one aliquot was heated to 95 °C for 5 min while the other aliquot directly subjected to SDS–PAGE.

When outer membrane  $\beta$ -barrel proteins are solubilized in SDS at moderate temperatures, they run on SDS–PAGE with an apparent molecular mass lower than that after incubation at 95 °C. The reason is that at lower temperatures the compact structure of a folded  $\beta$ -barrel protein is preserved despite the presence of SDS, thereby providing it with a faster electrophoretic mobility.<sup>27</sup> This so-called heat modifiability is a typical property of bacterial outer membrane proteins that allows an assessment of their folding state by SDS–PAGE.

Figure 2C shows the radioactively labeled TtoA following its *in vitro* synthesis and incubation with the indicated vesicles, separation by SDS–PAGE, and visualization by phosphoimaging. When TtoA was incubated with TtOmp85-containing proteoliposomes at 37 °C (lanes 5 and 6), a substantial fraction of TtoA had in fact become heat-modifiable. Thus, 28% of TtoA (means of three independent experiments) exhibited an accelerated electrophoretic mobility (black dot), provided that it was denatured at 22 °C instead of 95 °C.

A faint background band displaying an electrophoretic mobility similar to that of folded TtoA appeared in all samples treated at 95 °C (asterisk). If this band were related to folded TtoA, it would have become stronger at 22 °C, which definitely

was not the case (lanes 1 and 3). In contrast, the band labeled with the dot strictly required the presence of TtOmp85 (compare lanes 3 and 5) and was prominent only at 22 °C, indicating that this band in fact reflects folded TtoA. When the integration reaction was performed at 70 °C, which is the optimal living temperature of *T. thermophilus*, membrane integration, as indicated by folding, proceeded with a higher efficiency (42%; compare lanes 5 and 7). These findings clearly indicate that the observed folding of TtoA was the result of the activity of TtOmp85 and that purified TtOmp85 had been reconstituted in a functional manner.

**Only Peptides with the C-Terminal Amino Acid Sequences of TtoA Affect the Conductance of TtOmp85 Channels in BLM.**

To study the effect of peptide substrates on TtOmp85, we performed single-channel studies based on previously published results.<sup>13</sup> If  $\beta$ -strands of TtoA peptides are inserted into the TtOmp85 barrel, it may be expected that its single-channel conductance would be affected. Reliable information about such modifications of the TtOmp85 channel is, however, not obtained from a few single-channel events because the insertion of TtoA peptides is a stochastic process, even if the substrate is added in excess. Therefore, numerous membranes with TtOmp85 alone and with peptide substrates were measured and analyzed, and the resulting single-channel histograms were combined for each experimental condition separately to obtain at least 36000 events for each condition. To reveal possible modifications, histograms with and without added peptides were compared. For this purpose, the histograms were normalized with respect to the total number of events and overlaid. As will be shown below, significantly modified single-channel conductances were detected, but the larger fraction of ion channels was unmodified.

When purified TtOmp85 was added to one compartment of a BLM cuvette, single-channel current fluctuations were obtained at varying times after the addition. The reconstituted protein generated distinct current changes that represented opening and closing events of a channel, examples of which are shown in Figure 3. The current signals were converted to conductance

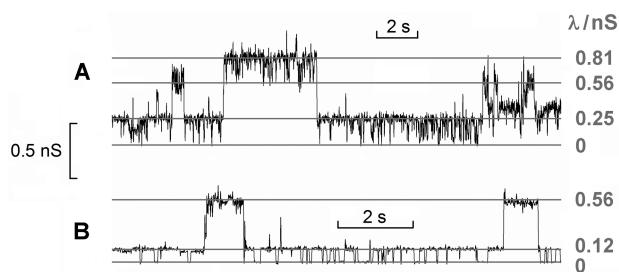


**Figure 3.** Conductance recordings of black lipid membranes containing TtOmp85 showing stepwise changes in current caused by channel opening and closing. The recorded current was divided by the applied membrane voltage ( $V_M = 100$  mV) to obtain conductance  $\lambda$  as the ordinate. Two typical recordings of a single channel, A and B, are shown with characteristic conductance levels between 0.12 and 0.81 nS (1 M KCl;  $T = 20$  °C).

values for display. Recordings with more than one channel were discarded. Once a channel appeared, a number of different conductance levels,  $\lambda$ , were reproducibly observed. The  $\lambda$  levels remained invariant until the channel activity ended or the membrane broke and were reproducible in different membranes. Transitions were observed between various conductance levels. The conductance changes will be denoted in the following as  $\Lambda$ .

Values of  $\Lambda$  obtained from the same scan are 0.12, 0.25, 0.31, and 0.44 nS, with various successive transitions (Figure 3). This observation indicates that the conductance transitions did not result from two or more successive channel insertion events. However, the recordings do not allow per se discrimination between two possibilities. A single channel with more than one conducting states could produce these transitions, or a single oligomer of channel proteins could exhibit a superposition of their conductances. The latter case is, however, unlikely because the monomeric nature of TtOmp85 was recently confirmed by various techniques.<sup>13</sup>

Open-channel states lasted for intervals from <1 ms to a maximum of 6 s. At open states with a conductance level of  $\geq 0.25$  nS, frequent flickering was observed with amplitudes of <0.25 nS (Figure 3A), which partially were so short that they may not have been resolved completely because of the limited time resolution of the setup. This behavior indicates fractional interruptions of the open states. The histogram of conductance transitions  $\Lambda$  of TtOmp85 from more than 15 independent BLM experiments containing more than 140000 events is shown in Figure 5A. The maximum in the range between 0.15 and 0.25 nS preferentially represents the flickering behavior of the TtOmp85 channel mentioned above. The predominant peak at 0.4 nS published previously<sup>13</sup> is indicated by a shoulder in the histogram. The absence of a typical peak has to be explained by a superposition of the aforementioned numerous conductance transitions and the width of their distribution. No open-channel events were observed in the presence of detergent only (0.05% Cymal-6) or in the presence of full-length TtoA or the TtoA-derived peptides only (not shown).

To test the effect of substrates on the channels formed by TtOmp85, several TtoA-derived peptide fragments were designed (Figure 2 of the Supporting Information). B8 and B7-8 comprised the sequence of the C-terminal  $\beta$ -strands and the two C-terminal  $\beta$ -strands of TtoA, respectively, whereas B1 and B1-2 comprised those of the N-terminal  $\beta$ -strand sequence and the two N-terminal  $\beta$ -strands of TtoA, respectively. Each of these peptides was added in solubilized form mixed with TtOmp85 in a molar ratio of 5:1 and added to the BLM. Alternatively, the peptide and TtOmp85 were mixed in molar ratios of 1:1 before addition, or the peptide was added after single-channel events of TtOmp85 only were observed. The application methods had no significant effect on the observed single-channel conductances. Single-channel fluctuations were recorded from TtOmp85 with each peptide.

A characteristic feature of the channel formed by TtOmp85 and peptide B7-8 was a burst behavior (Figure 4). It was absent in TtOmp85-only recordings. Between phases of completely closed channels, the conductance switched quickly for up to minutes between several levels from 0.34 to  $\sim 1.4$  nS. When expanded, the distinct levels and transitions can be easily identified (Figure 4A,B). These transitions within one burst indicate that the conductance levels belong to the same channel molecule. The duration of particular levels varied between <1 ms and  $\sim 1$  s. As mentioned above, amplitudes of levels with a lifetime shorter than 2 ms may be incompletely resolved and contribute to a broadening of the conductance distribution in the histograms (Figure 5B).

When from the histogram obtained from TtOmp85 and peptide B7-8 (Figure 5B) the rescaled TtOmp85 histogram (Figure 5A) is subtracted in a way that the difference is minimized in the conductance region below 0.35 nS, the remaining conductance changes show a broad maximum in the range between 0.6 and 1.8 nS. They are assigned to additional conductance states induced by the interaction with B7-8. The

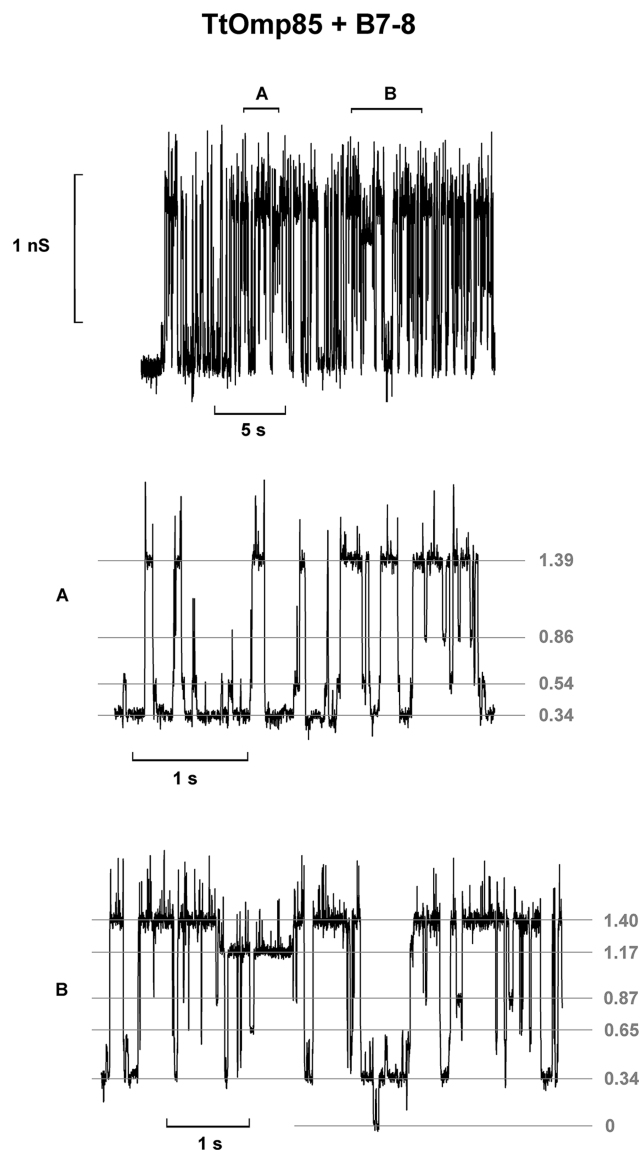


**Figure 4.** Single-channel conductance recordings of black lipid membranes containing TtOmp85 and peptide B7-8. The compound channel formed by TtOmp85 and B7-8 shows long-living bursts containing frequent transitions among at least five different conductance levels,  $\lambda$  (expanded in panels A and B). The other experimental conditions were like those described in the legend of Figure 3.

maximal changes scored at  $\sim 0.7$  nS (Figure 5B). TtOmp85-only channels showed almost no events above 0.7 nS [ $<0.2\%$  (Figure 5A)]. The “surplus” conductance events of the TtOmp85 and peptide B7-8 condition (8639 events) were  $\sim 11\%$  of the total count. This number indicates that the majority of recorded conductance transitions presumably were from unmodified TtOmp85 channels.

The histograms of the conductance transitions of the channel with the other peptides and TtoA are shown in Figure 5C–F. In each case, they were compared to the histogram of TtOmp85 to identify modifications of the single-channel conductances.

In the presence of B8 (Figure 5C), a small surplus cluster was found (2376 events,  $\sim 6.5\%$ ) at a single-channel conductance of  $0.7 \pm 0.2$  nS. In contrast, the addition of full-length TtoA protein (Figure 5D), of B1-2 (Figure 5E), and of B1 (Figure 5F) caused no significant modification of TtOmp85-channel conductance transitions.

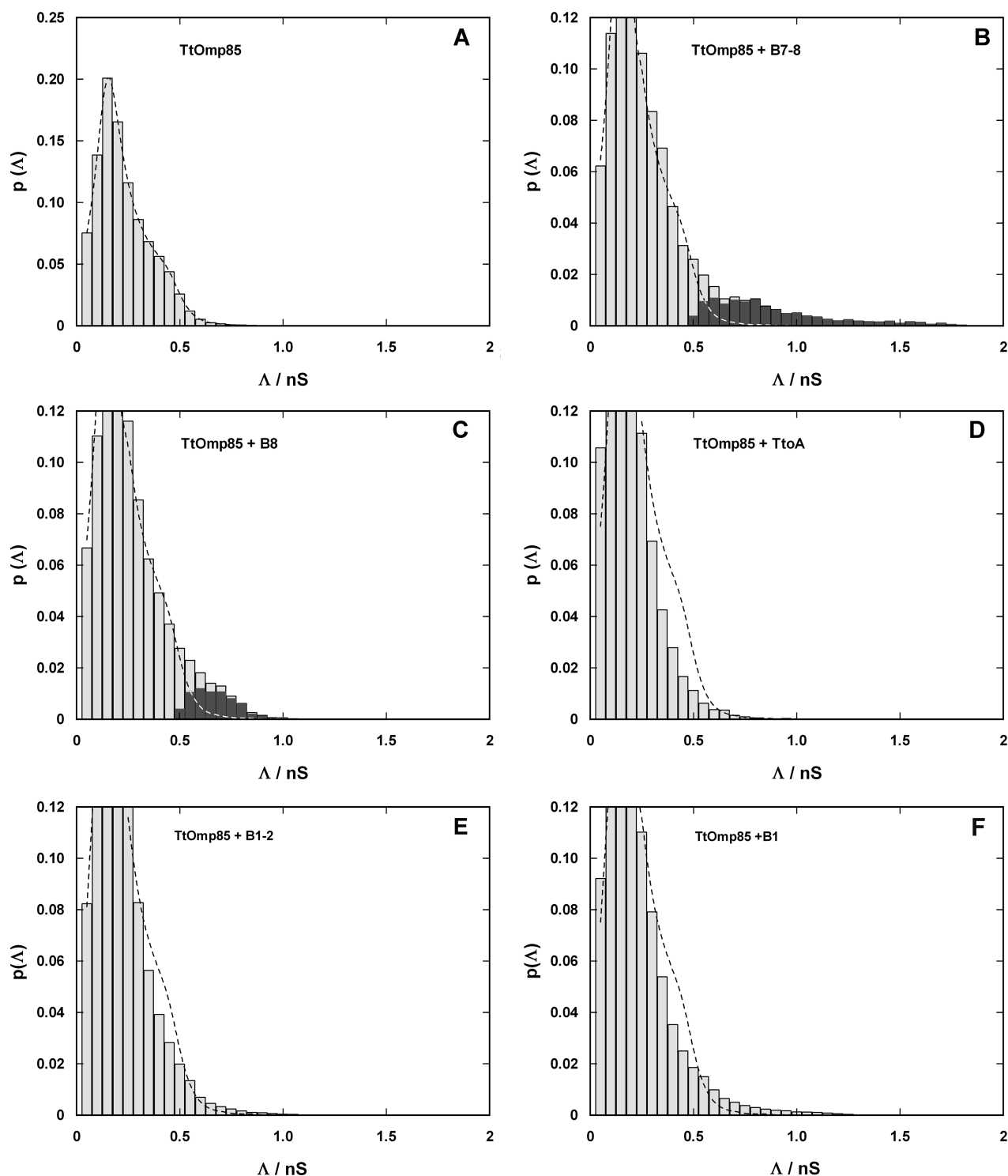


**Figure 5.** Histograms of single-channel conductance changes,  $\Delta$ , observed upon addition of TtOmp85 and the indicated peptides to the BLM: (A) TtOmp85 alone, 145501 events; (B) TtOmp85 with peptide B7-8, 77672 events; (C) TtOmp85 with peptide B8, 36578 events; (D) TtOmp85 with full-length TtoA, 13479 events; (E) TtOmp85 with peptide B1-2, 234922 events; and (F) TtOmp85 with peptide B1, 218197 events. The envelope of the histogram of the TtOmp85-only channels shown in panel A is represented as a dashed line in all panels for comparison. In panels B and C, the difference between the histograms of TtOmp85 with and without added peptide was significant above 0.5 nS and is shown as dark gray bars that correspond to the larger  $\Delta$  values found in the recordings of Figure 4. Addition of peptides B1, B1-2, and full-length TtoA did not produce significant amounts of conductance changes in addition to that of TtOmp85 alone.

## DISCUSSION

An inspection of the sequence of TtOmp85 shows that it shares all typical characteristics with other members of the Omp85 family. It possesses six N-terminal POTRA domains<sup>28</sup> and a C-terminal

16-strand transmembrane barrel domain that, compared with porin barrels, has a reduced interaction energy of its first and 16th strands similar to what was revealed by the known crystal structures.<sup>11,12</sup>

The insertase function of TtOmp85 has been confirmed here by an *in vitro* experiment that showed that TtOmp85 mediates

insertion of TtoA into liposomes in a heat-modifiable manner. Thus, TtOmp85 is a functional representative of the Omp85 protein family even though *T. thermophilus* is an ancient member of eubacteria, an intermediate between Gram-positive and Gram-negative bacteria<sup>14</sup> possessing glycolipids instead of lipopolysaccharides. The evolutionary distance to the *E. coli* Bam system is also indicated by the failure to find homologues of accessory BamB–BamE proteins in the *T. thermophilus* genome. Consistent with the absence of the accessory Bam components, the *in vitro* reconstitution of the membrane insertion required only the BamA ortholog TtOmp85, and because of this, simplicity should facilitate the investigation of the insertion mechanism of  $\beta$ -barrel OMPs.<sup>29</sup>

Kim et al.<sup>30</sup> and Knowles et al.<sup>31</sup> proposed that partially folded OMPs dock to POTRA domains of YaeT via interprotein  $\beta$ -augmentation whereby a  $\beta$ -strand of an unfolded substrate protein binds to a solvent-exposed face of a  $\beta$ -strand of a POTRA domain. From there, it is guided further toward the outer membrane.

Questions about whether during the insertase cycle the transmembrane barrel would act as a rigid scaffold, act as a monomer or oligomer, or be even more actively involved by going through a cycle of conformations during membrane insertion of a substrate outer membrane  $\beta$ -barrel protein arose.

Robert et al.<sup>7</sup> recorded BLM conductance with an Omp85 protein and found conductance levels comparable to those reported here. They interpreted the levels as combinations of opened and closed monomers in a tetramer and suggested that this is the functional oligomer of the insertase. Because of evidence of a monomeric TtOmp85 organization<sup>13</sup> and the known crystal structures, we rather interpret the conductance levels as arising from the same insertase monomer. The channel conductance transitions of TtOmp85 in our experiments were not distributed around a single, distinct peak value possibly because of the superposition of open states that range from rather constricted to more dilated ion pathways, generating a kind of continuous distribution.

To assess the involvement of the transmembrane  $\beta$ -barrel of TtOmp85 in the assembly process of TtoA, we recorded conductance in the absence and presence of four TtoA-derived peptides. In the presence of the C-terminal TtoA peptides, we observed additional channel conductance levels that peaked in the transition conductance histograms at around  $0.7 \pm 0.2$  nS (in the case of B8) and between 0.6 and 1 nS (in the case of B7-8), i.e., partially at  $\Lambda$  values larger than those from TtOmp85 alone. The peptides thus not only dock to the POTRA domains but also enter the transmembrane part and enlarge the barrel cross section. The crystal structures of three Omp85 members<sup>11,12</sup> revealed a weak interaction between the first and 16th barrel strands because of a short 16th  $\beta$ -strand. Our theoretical calculations indicate that this is also the case for TtOmp85 and that this distinguishes the Omp85 insertase family from porins that shares with them a 16-strand transmembrane  $\beta$ -barrel. A  $\beta$ -augmentation of the opened TtOmp85 barrel at its first strand by B8 and B7-8 thus seems to be the most likely explanation. Assuming the simplest case of a cylindrical barrel with a completely open inside, the cross-sectional ratio for two water-filled cylindrical barrel channels with 18 and 17 strands would be 1/0.89. The ratio of both conductance values (1.0/0.7) is, however, larger than the predicted value. The failure of this simple model indicates that formation of the complex between TtOmp85 and the peptides must affect other parts of the TtOmp85 barrel structure, as well. In the presence of the

peptides, we observed long-living burst periods (up to minutes). During such extended periods, the compound channel switches on a millisecond to second scale frequently between high and low conductance levels. While high conductance levels likely represent a channel with a large cross section at its constriction site, the low-conductance states must not necessarily represent a channel squeezed at a constriction site but could also be caused by an unfavorable positioning of polar residues elsewhere in the ion pathway. We propose that the barrel cross section is rather invariant during the burst periods but the loops and/or POTRA domains assume several alternative conformations that modulate the conductance. Similar bursts are seen in conductance recordings of the trimeric maltoporin in the presence of maltohexaose in ref 32. This concept supports the view of a dynamic but long-living complex in which TtoA peptides augment the transmembrane barrel of TtOmp85. The observed bursts could reflect fast conformational transitions that allow the sampling of different patterns of hydrogen bonds between the TtoA strands themselves and the contacting Omp85 strand. Such an ensemble of different strand associations that interconvert frequently into each other may be needed to allow for sliding of the strands along each other toward an energetically favorable folding intermediate rather than being trapped into a local, kinetically stable, free energy minimum. In presence of the B1 and B1-2 peptides, we did not observe channels other than those of TtOmp85 alone (Figure 5 E,F). This finding confirms reports<sup>7,33</sup> that show that compound channels form only in the presence of substrate-derived peptides that contain the C-terminal recognition sequence.

Formation of  $\beta$ -sheets across protein–protein interfaces has been previously reported in other protein complexes<sup>34,35</sup> and in  $\beta$ -strand domain swapping<sup>36</sup> and in crystal contacts.<sup>6</sup>

While formation of a  $\beta$ -sheet by simultaneous association of several single strands or several hairpins appears to be unlikely and will be inhibited kinetically, association of further strands to a preexisting sheet nucleus is favored by the cooperativity of hydrogen bonds as shown for a model peptide that forms amyloid-like fibers.<sup>37</sup> To overcome the initial barrier of forming a two- or three-stranded  $\beta$ -sheet,  $\beta$ -augmentation would be a catalytic solution. Furthermore, the aqueous channel of TtOmp85 will reduce the energetic barrier of translocation of the polar extracellular loops of the substrate OMP.

**A Hypothetical Course of the Insertase Cycle.** One  $\beta$ -strand or a  $\beta$ -hairpin of the unfolded TtoA protein could be associated weakly with a POTRA domain so that a transfer to the transiently open TtOmp85 barrel would be energetically favorable and kinetically possible. The POTRA domain might function as a slide for TtoA into the TtOmp85 barrel. The reduced dielectric constant in the membrane will stabilize hydrogen bonds<sup>38,39</sup> and contribute to a favorable energy of formation of the new intermolecular  $\beta$ -sheet.  $\beta$ -Augmentation by transfer of TtoA  $\beta$ -strands may then occur at the first TtOmp85 strand because it is longer than strand 16.<sup>11,12</sup> The C-terminal eighth strand of TtoA should associate with it, succeeded by the seventh (see Figure 6). The apolar surface of the growing TtoA barrel would be oriented toward the membrane, which is favored by hydrophobic interactions.

A large amount of strain energy will not accumulate in the growing TtoA barrel as long as the number of inserted TtoA strands remains low because  $\beta$ -barrels are very permissive to curvature. Known outer membrane  $\beta$ -barrels have been found with an even number of strands between 8 and 22. Furthermore, twist, shear numbers, and lengths of  $\beta$ -strands of OMP barrel proteins resemble those of Omp85 proteins. When the site of

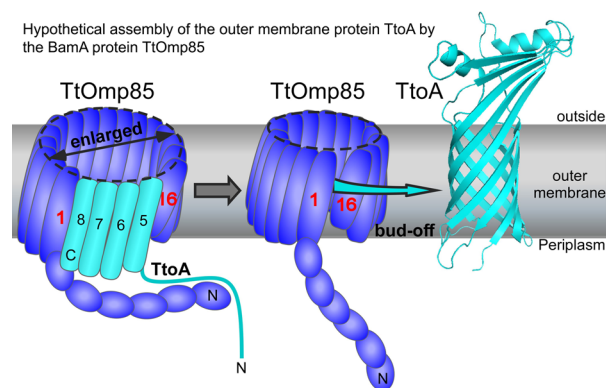


**Figure 6.** Scheme illustrating a hypothetical insertion mechanism for the TtOmp85 insertase. In the left panel, unfolded TtoA is bound to the POTRA domains of TtOmp85. The barrel of the insertase is closed. In the middle panel, the TtOmp85 barrel has opened and the  $\beta$ -sheet has been augmented at the first  $\beta$ -strand by four C-terminal  $\beta$ -strands of TtoA. The POTRA domains with the remaining unfolded N-terminal part of TtoA have pivoted toward the insertion site. In the right panel, folded TtoA has dissociated from TtOmp85.

insertion of TtoA OMP  $\beta$ -strands into the compound barrel is gradually stepping away from the first TtOmp85  $\beta$ -barrel strand, the POTRA domains might follow by pivoting with their attached TtoA strands to the actual site.

Beyond a certain number of inserted strands, the strain in the compound barrel could reach a critical threshold level so that the remaining strands would spontaneously insert and the full-length TtoA would bud off from TtOmp85 as an independent, closed eight-strand  $\beta$ -barrel. This could resemble the spontaneous completion of the 11-strand barrel of green fluorescent protein from a 10-strand fragment and the peptide of the 11th strand.<sup>40</sup>

A similar scenario was sketched for bacterial outer membrane  $\beta$ -barrel proteins by Kim et al.<sup>41</sup> and Stegmeier and Andersen.<sup>42</sup> The latter authors were to the best of our knowledge the first to propose that barrels of the Omp85 family might open so that folded OMP substrate barrels could be released laterally into the outer membrane.

## ■ ASSOCIATED CONTENT

### Supporting Information

Two figures of the predicted topology of the transmembrane strands of TtOmp85 and the topology of TtoA and one table indicating barrel-closure energies in selected porins and Omp85 proteins. This material is available free of charge via the Internet at <http://pubs.acs.org>.

## ■ AUTHOR INFORMATION

### Corresponding Author

\*Department of Biology, University of Konstanz, Universitätsstr. 10, 78457 Konstanz, Germany. E-mail: [wolfram.welte@uni-konstanz.de](mailto:wolfram.welte@uni-konstanz.de). Telephone: +497531882206. Fax: +497531883183.

### Funding

This work was funded by the Deutsche Forschungsgemeinschaft (Collaborative Research Center 969) and by NIH grant GM079804.

### Notes

The authors declare no competing financial interest.

## ■ ABBREVIATIONS

BLM, black lipid membrane(s); OMPs, integral outer membrane proteins; PTB, protein-transporting  $\beta$ -barrel proteins; POTRA,

polypeptide transport-associated domains; TtoA, *T. thermophilus* outer membrane protein A; PF-MS, peptide fragment mass spectrometry; PhPC, L-1,2-diphytanoyl-3-phosphatidylcholine.

## ■ REFERENCES

- (1) Wimley, W. C. (2003) The versatile  $\beta$ -barrel membrane protein. *Curr. Opin. Struct. Biol.* 13, 404–411.
- (2) Kleinschmidt, J. H., den, B. T., Driessen, A. J., and Tamm, L. K. (1999) Outer membrane protein A of *Escherichia coli* inserts and folds into lipid bilayers by a concerted mechanism. *Biochemistry* 38, 5006–5016.
- (3) Voulhoux, R., Bos, M. P., Geurtsen, J., Mols, M., and Tommassen, J. (2003) Role of a highly conserved bacterial protein in outer membrane protein assembly. *Science* 299, 262–265.
- (4) Walther, D. M., Rapaport, D., and Tommassen, J. (2009) Biogenesis of  $\beta$ -barrel membrane proteins in bacteria and eukaryotes: Evolutionary conservation and divergence. *Cell. Mol. Life Sci.* 66, 2789–2804.
- (5) Struyvé, M., Moons, M., and Tommassen, J. (1991) Carboxy-terminal phenylalanine is essential for the correct assembly of a bacterial outer membrane protein. *J. Mol. Biol.* 218, 141–148.
- (6) Brosig, A., Nesper, J., Boos, W., Welte, W., and Diederichs, K. (2009) Crystal structure of a major outer membrane protein from *Thermus thermophilus* HB27. *J. Mol. Biol.* 385, 1445–1455.
- (7) Robert, V., Volokhina, E. B., Senf, F., Bos, M. P., Van, G. P., and Tommassen, J. (2006) Assembly factor Omp85 recognizes its outer membrane protein substrates by a species-specific C-terminal motif. *PLoS Biol.* 4, e377.
- (8) Jacob-Dubuisson, F., Villeret, V., Clantin, B., Delattre, A. S., and Saint, N. (2009) First structural insights into the TpsB/Omp85 superfamily. *Biol. Chem.* 390, 675–684.
- (9) Sanchez-Pulido, L., Devos, D., Genevrois, S., Vicente, M., and Valencia, A. (2003) POTRA: A conserved domain in the FtsQ family and a class of  $\beta$ -barrel outer membrane proteins. *Trends Biochem. Sci.* 28, 523–526.
- (10) Bos, M. P., Robert, V., and Tommassen, J. (2007) Functioning of outer membrane protein assembly factor Omp85 requires a single POTRA domain. *EMBO Rep.* 8, 1149–1154.
- (11) Noinaj, N., Kuszak, A. J., Gumbart, J. C., Lukacik, P., Chang, H., Easley, N. C., Lithgow, T., and Buchanan, S. K. (2013) Structural insight into the biogenesis of  $\beta$ -barrel membrane proteins. *Nature* 501, 385–390.
- (12) Gruss, F., Zahringer, F., Jakob, R. P., Burmann, B. M., Hiller, S., and Maier, T. (2013) The structural basis of autotransporter translocation by TamA. *Nat. Struct. Mol. Biol.* 20, 1318–1320.
- (13) Nesper, J., Brosig, A., Ringler, P., Patel, G. J., Muller, S. A., Kleinschmidt, J. H., Boos, W., Diederichs, K., and Welte, W. (2008) Omp85(T) from *Thermus thermophilus* HB27: An ancestral type of the Omp85 protein family. *J. Bacteriol.* 190, 4568–4575.
- (14) Acosta, F., Ferreras, E., and Berenguer, J. (2012) The  $\beta$ -barrel assembly machinery (BAM) is required for the assembly of a primitive S-layer protein in the ancient outer membrane of *Thermus thermophilus*. *Extremophiles* 16, 853–861.
- (15) Bagos, P. G., Liakopoulos, T. D., Spyropoulos, I. C., and Hamodrakas, S. J. (2004) PRED-TMBB: A web server for predicting the topology of  $\beta$ -barrel outer membrane proteins. *Nucleic Acids Res.* 32, W400–W404.
- (16) Ou, Y. Y., Chen, S. A., and Gromiha, M. M. (2010) Prediction of membrane spanning segments and topology in  $\beta$ -barrel membrane proteins at better accuracy. *J. Comput. Chem.* 31, 217–223.
- (17) Buchan, D. W., Ward, S. M., Lobley, A. E., Nugent, T. C., Bryson, K., and Jones, D. T. (2010) Protein annotation and modelling servers at University College London. *Nucleic Acids Res.* 38, W563–W568.
- (18) Jackups, R., Jr., and Liang, J. (2005) Interstrand pairing patterns in  $\beta$ -barrel membrane proteins: The positive-outside rule, aromatic rescue, and strand registration prediction. *J. Mol. Biol.* 354, 979–993.
- (19) Naveed, H., Jackups, R., Jr., and Liang, J. (2009) Predicting weakly stable regions, oligomerization state, and protein-protein interfaces in



transmembrane domains of outer membrane proteins. *Proc. Natl. Acad. Sci. U.S.A.* 106, 12735–12740.

(20) Wouters, M. A., and Curmi, P. M. (1995) An analysis of side chain interactions and pair correlations within antiparallel  $\beta$ -sheets: The differences between backbone hydrogen-bonded and non-hydrogen-bonded residue pairs. *Proteins* 22, 119–131.

(21) Brosig, A., Nesper, J., Welte, W., and Diederichs, K. (2008) Expression, crystallization and preliminary X-ray analysis of an outer membrane protein from *Thermus thermophilus* HB27. *Acta Crystallogr. F* 64, 533–536.

(22) Laemmli, U. K. (1970) Cleavage of structural proteins during the assembly of the head of bacteriophage T4. *Nature* 227, 680–685.

(23) Smith, P. K., Krohn, R. L., Hermanson, G. T., Mallia, A. K., Gartner, F. H., Provenzano, M. D., Fujimoto, E. K., Goeke, N. M., Olson, B. J., and Klenk, D. C. (1985) Measurement of protein using bicinchoninic acid. *Anal. Biochem.* 150, 76–85.

(24) Moser, M., Panahandeh, S., Holzapfel, E., and Müller, M. (2007) In vitro analysis of the bacterial twin-arginine-dependent protein export. *Methods Mol. Biol.* 390, 63–79.

(25) Fan, E., Fiedler, S., Jacob-Dubuisson, F., and Müller, M. (2012) Two-partner secretion of Gram-negative bacteria: A single  $\beta$ -barrel protein enables transport across the outer membrane. *J. Biol. Chem.* 287, 2591–2599.

(26) Läger, P., Lesslauer, W., Marti, E., and Richter, J. (1967) Electrical properties of bimolecular phospholipid membranes. *Biochim. Biophys. Acta* 135, 20–32.

(27) Rosenbusch, J. P. (1974) Characterization of the major envelope protein from *Escherichia coli*. Regular arrangement on the peptidoglycan and unusual dodecyl sulfate binding. *J. Biol. Chem.* 249, 8019–8029.

(28) Arnold, T., Zeth, K., and Linke, D. (2010) Omp85 from the thermophilic cyanobacterium *Thermosynechococcus elongatus* differs from proteobacterial Omp85 in structure and domain composition. *J. Biol. Chem.* 285, 18003–18015.

(29) Leone, S., Molinaro, A., Lindner, B., Romano, I., Nicolaus, B., Parrilli, M., Lanzetta, R., and Holst, O. (2006) The structures of glycolipids isolated from the highly thermophilic bacterium *Thermus thermophilus* Samu-SA1. *Glycobiology* 16, 766–775.

(30) Kim, K. H., Aulakh, S., and Paetzel, M. (2012) The bacterial outer membrane  $\beta$ -barrel assembly machinery. *Protein Sci.* 21, 751–768.

(31) Knowles, T. J., Jeeves, M., Bobat, S., Dancea, F., McClelland, D., Palmer, T., Overduin, M., and Henderson, I. R. (2008) Fold and function of polypeptide transport-associated domains responsible for delivering unfolded proteins to membranes. *Mol. Microbiol.* 68, 1216–1227.

(32) Kullman, L., Winterhalter, M., and Bezrukov, S. M. (2002) Transport of maltodextrins through maltoporin: A single-channel study. *Biophys. J.* 82, 803–812.

(33) Kutik, S., Stojanovski, D., Becker, L., Becker, T., Meinecke, M., Kruger, V., Prinz, C., Meisinger, C., Guiard, B., Wagner, R., Pfanner, N., and Wiedemann, N. (2008) Dissecting membrane insertion of mitochondrial  $\beta$ -barrel proteins. *Cell* 132, 1011–1024.

(34) Remaut, H., and Waksman, G. (2006) Protein-protein interaction through  $\beta$ -strand addition. *Trends Biochem. Sci.* 31, 436–444.

(35) Harrison, S. C. (1996) Peptide-surface association: The case of PDZ and PTB domains. *Cell* 86, 341–343.

(36) Ködding, J., Killig, F., Polzer, P., Howard, S. P., Diederichs, K., and Welte, W. (2005) Crystal structure of a 92-residue C-terminal fragment of TonB from *Escherichia coli* reveals significant conformational changes compared to structures of smaller TonB fragments. *J. Biol. Chem.* 280, 3022–3028.

(37) Tsemekhman, K., Goldschmidt, L., Eisenberg, D., and Baker, D. (2007) Cooperative hydrogen bonding in amyloid formation. *Protein Sci.* 16, 761–764.

(38) Wimley, W. C., Hristova, K., Ladokhin, A. S., Silvestro, L., Axelsen, P. H., and White, S. H. (1998) Folding of  $\beta$ -sheet membrane proteins: A hydrophobic hexapeptide model. *J. Mol. Biol.* 277, 1091–1110.

(39) White, S. H. (2006) How hydrogen bonds shape membrane protein structure. *Adv. Protein Chem.* 72, 157–172.

(40) Cabantous, S., Terwilliger, T. C., and Waldo, G. S. (2005) Protein tagging and detection with engineered self-assembling fragments of green fluorescent protein. *Nat. Biotechnol.* 23, 102–107.

(41) Kim, K. H., Aulakh, S., and Paetzel, M. (2012) The bacterial outer membrane  $\beta$ -barrel assembly machinery. *Protein Sci.* 21, 751–768.

(42) Stegmeier, J. F., and Andersen, C. (2006) Characterization of pores formed by YaeT (Omp85) from *Escherichia coli*. *J. Biochem.* 140, 275–283.